Juniper Online
Journal Material Science
ISSN: 2575-856X

Research Article
Volume 6 Issue 4- August 2021
DOI: 10.19080/JOJMS.2021.06.555693

JOJ Material Sci

A New Method for Simultaneously Testing Fracture Brittleness and Conductivity

Zhengwen Zeng* and Abdallah Harouaka

Department of Petroleum Engineering, University of Texas Permian Basin, Midland, TX 79705, USA

Submitted: July 26, 2021; **Published:** August 11, 2021

***Corresponding author:** Zhengwen Zeng, Department of Petroleum Engineering, University of Texas Permian Basin, Midland, TX 79705, USA

Abstract

Multistage hydraulic fracturing of horizontal wells is the prevailing technology for developing unconventional hydrocarbon reserves like the Wolfcamp tight formation in the Permian Basin, USA. Hydraulic fracturing treatment assumes the stimulation will create brittle and conductive fractures in all clusters of each stage. The stimulation outcome with respect to fracture brittleness and the scope of fracture conductivity should be determined experimentally and simultaneously. To our knowledge, existing technologies test fracture brittleness and fracture conductivity separately. This paper introduces a new method that measures fracture brittleness and fracture conductivity simultaneously. Testing results on Testing results on Indianan limestone show that: (1) Confining pressure is a dominant factor in controlling whether the rock fractures in brittle mode or fails in ductile mode. (2) If the rock fractures in a brittle mode, the rock matrix permeability, and subsequently the fracture conductivity increases rapidly during and post fracturing/failing process. (3) If the rock fails in a ductile mode, matrix permeability decreases monotonically before, during and post the fracturing process. (4) Transitional behaviors have been observed when the rock fails between semi-brittle and semi-ductile modes under an intermediate range of confining pressures. The latter corresponds to reservoir conditions in most of the real world cases. (5) The new testing has shown it can provide means to increase the possibility of creating brittle and conductive fractures.

Keywords: Multistage hydraulic fracturing; Horizontal wells; Tight oil reservoir stimulation; Fracture brittleness and conductivity; Brittle-ductile transition

Abbreviations: API: American Petroleum Institute; BPR: Back Pressure Regulator; D.I. Water: De-Ionized Water; DOE: Department of Energy (USA); FRID: Fluid-Rock Interaction Dynamics; HD: Horizontal Drilling; HDHF: Horizontal Drilling and Multistage Hydraulic Fracturing; HF: Hydraulic Fracturing; ID: Identification (Sample ID); ISO: International Standard Organization; ISRM: International Society for Rock Mechanics; mD: milli-Darcy, unit of permeability; ml: milliliter, unit of fluid volume; NETL: National Energy Technology Laboratories (USA); PC: Personal Computer; psi: pound per square inch, unit of stress and pressure; R&D: Research and Development; USD: US Dollar; USSR: the Union of Soviet Socialist Republics

Introduction

The US government established the Department of Energy (DOE) primarily as a response to the energy crisis of the 1970s. Through an elaborate financial support to research & development (R&D) several activities were undertaken leading to exploration and development of unconventional hydrocarbon resources [1]. After several decades of continuous efforts and hard work spectacular progresses were achieved. These progresses were also achieved through a judicious funding partnership by public and private sectors leading researchers in the industry, national labs and universities to the results everyone knows: The US has huge volumes of oil and natural gas in unconventional formations [2,3]. With new completion techniques, combining horizontal drilling with multistage hydraulic fracturing (HDHF), these unconventional oil and gas resources can be technically and commercially produced [4,5].

The "discovery" of hydraulic fracturing (HF) was a side product of a cement squeezing operation in the 1940s [6]. It was subsequently improved and applied to enhance production via intentionally breaking reservoir rocks to overcome near wellbore damage and to increase drainage volume through creating highly conductive hydraulic fractures in low permeability formations [7,8]. In developing conventional oil and gas resources, HF

technology has been employed mainly to create fractures in vertical wells [9].

Horizontally drilled wells (HD) can increase the contact area between wellbore and the reservoir. This becomes quite important when producing from thin pay zones, which led to several US trials in the 1940s [10] as well as in the USSR in the 1950s [11]. However, the first horizontal wells economic production took place in heavy oil Canadian fields [10]. The prodigious success of horizontal wells in the Austin chalk, a naturally fractured formation, hasted its wide application worldwide [12]. In the 1990s, horizontal wells were mainly used to increase oil and gas production in naturally fractured reservoirs and in some locations of restricted access. Horizontal wells can increase the contact area between wellbores and reservoirs.

The combination of HF and HD further increases the contact areas and drainage volumes in hydrocarbon reservoirs. Henceforth, it became logical to combine them for synergic effect [13]. However, initiating an HF in a horizontal well is much more complicated than doing so in a vertical well [14]. Theoretical and experimental studies have shown that HF initiation is controlled by local stress field [15], and its propagation is governed by far field stresses [16]. In addition to technical challenges, economics was another factor affecting the combined application of both technologies. Finally, in the late 1980s technical progresses and market factors were both favorable for people to reconvene discussions about the combined application of these two technologies, which eventually led to the initial success of HDHF in Barnette formation in 2003 [17]. Creating highly conductive hydraulic fractures is the key to commercially successful applications of HDHF technology. This is especially important to the development of unconventional resources where huge investment is generally involved along with extremely low matrix permeability in the source and reservoir rocks. Whether a hydraulic fracture is conductive or not depends heavily on fracture brittleness and/or failure mode by which the fracture is initiated. Hydraulic fractures initiated in brittle mode are in general much more conductive than those created otherwise.

Hydraulic fracturing treatment includes two major steps: Step 1 is to initiate the fractures using low viscosity pad fluid, such as slick water; and Step 2 is to propagate the pad fractures from the near wellbore region to the far field region in the reservoir using high viscosity fracturing fluid (slurry) that can carry proppants to the tip of fractures. Proppants keep fractures open after the fracturing fluid is flowed back. Fractures initiated in brittle mode allow the maximum transport of the fracturing slurry and proppants from the wellbore through the perforations to the fracture tips. In contrast, fractures initiated in semi-brittle/semi-ductile mode would more likely lead to early screen out owing to the inherent limited fracture conductivity.

Initiating a brittle fracture involves the favorable combination and interaction among four major factors: rock properties, in-situ stresses along with pore pressures, the pad fluid and the injection operations. Although many efforts have been made to find the brittle sections of rock formations using a variety of brittleness index definitions [18], initiating a brittle fracture is still not guaranteed. In fact, some of the unsuccessful HF stimulation jobs are attributed to the lack of brittle fractures [5], each of which could cost several million US dollars (USD). The objective of this paper is to introduce a new testing method capable of simultaneously measuring both fracture brittleness and conductivity.

Background

Hydraulic fracturing has been widely used in the petroleum industry since the late 1940s [19]. Various supporting testing technologies have been developed since then [20-22].

Rock fracture brittleness and failure mode

In mining and other related studies, rock strengths were measured by axially compressing the specimen to fail under constant confining pressures [23]. As early as 1945 Terzaghi observed that rock fails by splitting, shearing or pseudo shearing, depending on the inclination of the failure planes. Splitting represents cracking along the axial loading direction which causes bonds between mineral grains to fail due to lateral tension; shearing is due to displacement of grains along a gliding plane (shear plane); and pseudo shearing is the combination of the two that results in a "zig-zag" failure plane [24].

Griggs and Handin classified rock failure under room temperature and different combinations of axial and radial stresses into brittle and ductile [25]. They correlated each failure mode based on their stress-strain curves and their ultimate strains. According to that classification, rocks can undergo, from brittle splitting at ultimate strain below 1%, to ductile flowing/swelling at ultimate strain larger than 10%. Further investigation shows that a rock's failure mode is controlled by:

a) rock matrix structures,

b) magnitude of confining pressure,

c) temperature,

d) rate of loading, and

e) the nature of interstitial fluids [26].

"Brittleness" has been widely used to characterize reservoir rock in recent years [18]. Laboratory testing show that the same rock could behave in brittle or ductile mode, depending on other factors, such as confining pressure and temperature. For hydraulic fracturing application, it is preferred to reserve the term "brittleness" for fracture and the fracturing process [23]. If the rock fails in brittle mode, it creates a brittle and conductive fractures; if it fails in ductile mode, it generates ductile and less-/non-permeable compaction bands. On the stress-strain curve a brittle fracturing is featured by an obvious strength peak, followed by rapid loss of strength in the post-failure (post-peak) stage; in contrast, a ductile failure is featured by no strength peak followed

How to cite this article: Zeng Z, Harouaka A. A New Method for Simultaneously Testing Fracture Brittleness and Conductivity. JOJ Material Sci. 2021; 6(4): 555693. DOI: 10.19080/JOJMS.2021.06.555693

by gradual gain of strength in the post-failure stage; in-between exist semi-brittle and semi-ductile modes [22].

Because of these distinguishing features on the post-failure stress-strain curve, Jaeger and Cook proposed using the post-failure slope to quantify fracture brittleness [23]. Oil reservoir rocks are subjected to the combined total stresses of overburden and horizontal tectonic movements, and pore pressure from hydrocarbon fluids and salty water. They have been in equilibrium for thousands of years after the oil generating and migrating processes. When this equilibrium is disturbed due to drilling and production activities, reservoir rocks will respond through deformation, and sometimes failure, to reach new equilibrium. Rock deformation is proportional to the effective stresses, i.e. the net stresses on the rock matrix, which can be approximated as the differences between the total stresses and the pore pressure for permeable rocks [27]. When the combination of the effective stresses meet certain failure criterion, rock starts to fail following the corresponding mode, i.e., shearing slide, tensile breaking, or combination of both [28].

In HDHF completion, drilling teams may choose to place the well in the direction that is parallel to the minimum horizontal stress. Wellbores in the minimum horizontal stress direction allow completion teams to create multiple transverse fractures in the direction that is perpendicular to the wellbore axis. This is the prevailing practice in the present application of HDHF technology in order to generate maximum drainage volume in the reservoir via connecting existing natural fractures and directly contacting matrix rocks. Figure 1 shows the impact of wellbore direction on the initiated fractures in HDHF completion [29].

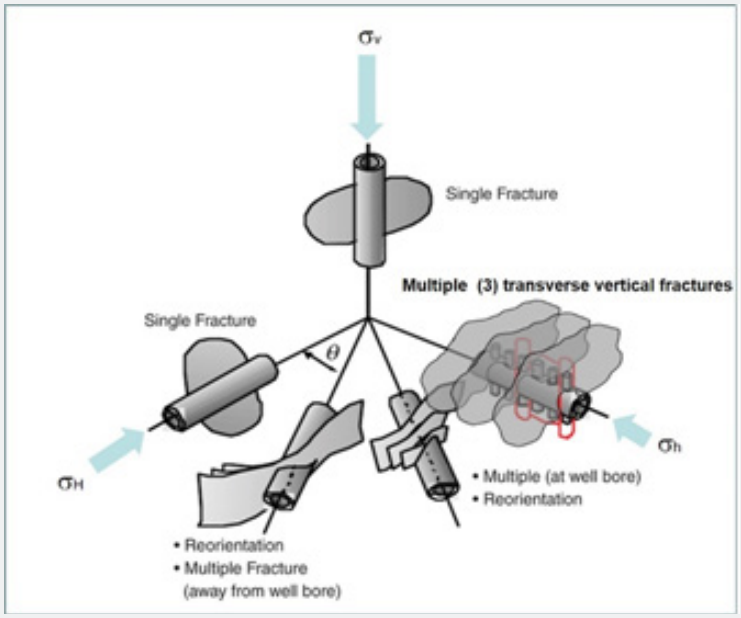

Figure 1: Impact of wellbore orientations on initiating hydraulic fractures [29].

Rock failure under tension in HF

During HF operation, the rock is under fixed total in-situ stress conditions. Injected HF fluids increase the pore pressure and reduce the effective stresses until conditions meet the rock's failure criterion. Depending on the orientation of the perforation and the local stress field near the wellbore, the failure could be brittle (breaking down, shearing) or ductile (flowing, swelling). Due to the complexity of the near wellbore stress field and the softening effect on the rock by the pad fluid, the uncertainty of initiating a brittle fracture in the reservoir tight rock is greatly increased. Before any field HF operations, it is better to conduct laboratory tests to verify and improve the design under controllable conditions to increase the certainty of initiating a brittle fracture.

HF breakdown pressure and laboratory test

HF breakdown pressure refers to the pressure at which the rock will fracture. It is measured under given stress conditions using a poly-axial block test [30,31]. This data is useful for estimating field breakdown pressure and for preparing the adequate pumping capacity in the field. Laboratory tests to measure the breakdown pressure require large rock blocks. The test is time consuming and requires advanced poly-axial rock mechanics testing facilities. Because of all these constraints, breakdown pressures are generally estimated using analytical solutions from other parameters [28].

Matrix permeability and fracture conductivity tests

In HF stimulation, matrix permeability represents how fast the reservoir rock can supply fluids to the fracture; and

How to cite this article: Zeng Z, Harouaka A. A New Method for Simultaneously Testing Fracture Brittleness and Conductivity. JOJ Material Sci. 2021; 6(4): 555693. DOI: 10.19080/JOJMS.2021.06.555693

fracture conductivity describes how fast the HF can transmit the reservoir fluids to the wellbore. The ideal case is achieved when the fracture conductivity matches the matrix permeability so fluids coming from the matrix will flow to the wellbore via the fracture promptly, and, on the other hand, the HF capacity could be fully utilized. Matrix permeability is routinely measured using reservoir rock specimens in a core-holder [32]. On the other hand, fracture conductivity is measured following API/ISO standards by packing one or more layer(s) of proppants in two artificially cut rock plates [33]. Because of the close relationship between matrix permeability and the fracture conductivity, it is ideal to measure the two in the same test simultaneously, instead of two separated ones. More importantly, the HF created fracture surfaces would be quite different from the surfaces of the two artificially cut rock plates. Therefore, it would be much more representative to measure the fracture conductivity from hydraulically created fracture surfaces.

Methodology

This section gives a brief description of the new testing technique, including hardware configuration, loading and control of axial and radial stresses (i.e. confining pressure) as well as pore pressure, and pore fluid flow, as well as related measurements.

Hardware configuration

The new laboratory testing technology is developed to increase the likelihood of creating a brittle and conductive fracture, and to reduce the possibilities of initiating a ductile failure in the field. During the rock failing/fracturing process under given reservoir stress conditions, axial stress-strain curve and axial matrix permeability are measured simultaneously. The axial-stress-strain curve is used to assess the fracture brittleness. The companion matrix permeability, and later, fracture conductivity, is used to quantify the effectiveness of the stimulation.

In an HF stimulation operation, the following are given conditions that will not be changed:

a) Reservoir rocks,

b) Formation fluids,

c) Reservoir temperature,

d) Total in-situ stresses, and

e) Pore pressure.

The following are controllable variables that can be adjusted for optimal HF results:

a) Wellbore orientation with respect to the in-situ stresses,

b) Perforation orientation with respect to the in-situ stresses,

c) Pad fluids, and

d) Loading rate of HF pressure.

The new testing technology and hardware facility, Figure 2, are based on the following existing laboratory testing technologies:

a) Poly-axial HF test [30,31],

b) Tri-axial geomechanics test [34], and

c) Tri-axial core flooding test [35].

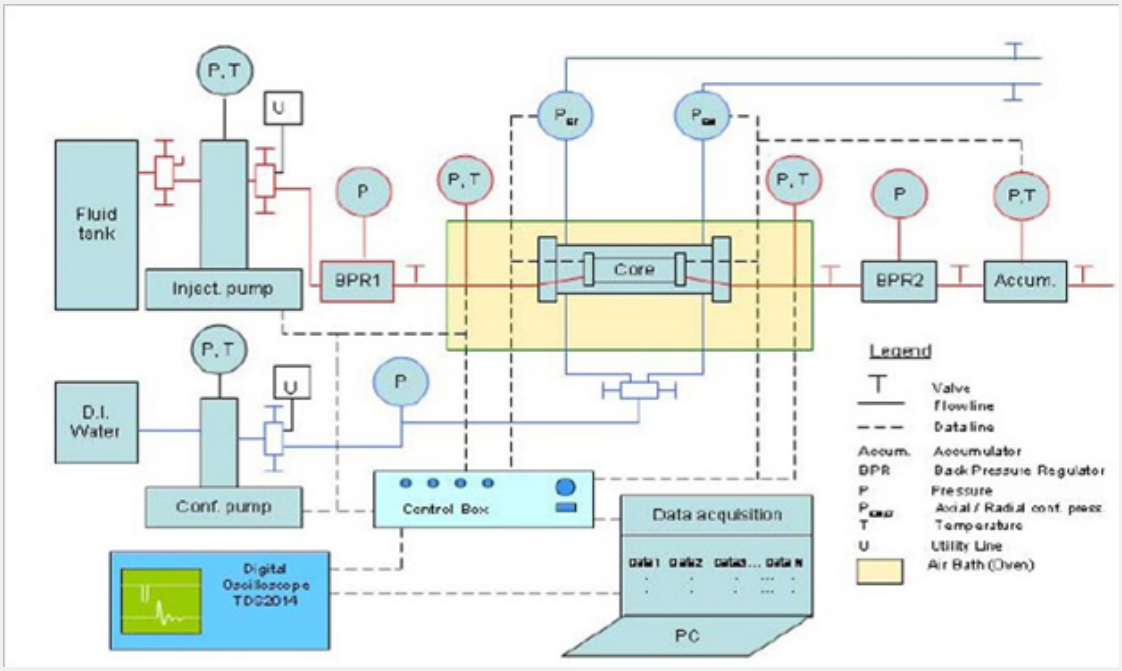

Figure 2: Diagram of the triaxial fracture brittleness and conductivity system [35].

How to cite this article: Zeng Z, Harouaka A. A New Method for Simultaneously Testing Fracture Brittleness and Conductivity. JOJ Material Sci. 2021; 6(4): 555693. DOI: 10.19080/JOJMS.2021.06.555693

Triaxial loading and compression

To investigate and demonstrate the impact of failure modes on matrix permeability and fracture conductivity, axial effective stress and permeability were simultaneously measured during the fracturing/failing process of six tests under different confining pressures. In-depth analyses of the time history of these axial stress and axial permeability allow the establishment of direct correlations between rock mechanical dynamics and fluid hydraulic dynamics under different conditions.

To catch the detailed dynamics of both brittle fracturing and ductile failing around the peak strength of the rock, the International Society for Rock Mechanics (ISRM) suggested a range of constant axial compression strain rate, i.e., 10^{-4} - 10^{-6} 1/s [36, 37]. In the fracture brittleness and conductivity tests shown below, rock sample axial deformation was achieved by pushing a 2.375-in diameter axial loading piston via injecting de-ionized water (D.I. water) into a 3.5-in diameter axial pressure chamber (Figure 3). A constant volumetric injection rate into the axial pressure chamber results in a constant axial compressional deformation rate, and consequently a constant axial compressive strain rate on the rock sample, assuming water compressibility is negligible. Therefore, the differential axial stress-time curve is equivalent to stress-strain curve obtained in standard rock mechanics test [23]. For 2-in long by 1-in diameter rock samples to be tested below, the volumetric injection rate corresponding to the ISRM suggested strain rates was 0.01 - 1.02 ml/min. To better depict the dynamic fracturing process especially under brittle mode, a volumetric injection rate of 0.02 ml/min was selected.

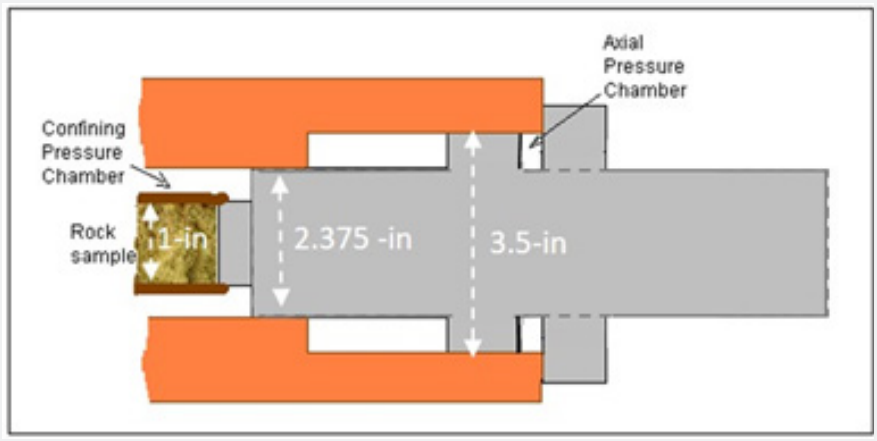

Figure 3: Diameters of rock sample (1-in), axial loading piston (2.375-in) and axial pressure chamber (3.5-in).

Fracture permeability measurement

Permeability measurement started at the initial pressurization stage. In these tests, the outlet backpressure regulator (BPR) was open to the air, meaning the reservoir bottom-hole pressure was set to 14.65 psi. An initial load of about 20 psi was applied to both axial and radial directions to drive the trapped air bubbles out and check the sealing. After the air bubbles were expelled and the sealing was secured, de-ionized water was injected through back pressure regulator 1 (BPR1) to the rock sample and exited through BPR 2 (Figure 2). Pressures in the upstream and downstream of the rock sample were measured. Injection rate of pore fluid is adjusted to such that a stabilized pressure difference of about 10 psi was achieved. Permeability was thus calculated based on Darcy's law. Once the stabilized injection was established, the axial flow was maintained in loading confining pressure and differential axial pressure, until the end of the test.

As the selected axial compressive strain rate was at the lower end of the ISRM recommended range [36, 37], it was assumed that steady-state flow in the rock sample continued and dominated the majority of the test, thus the measured permeability and its variation reflected the impact of the fracturing/failing process.

After the confining pressure was set, the valve connecting the radial and axial pressures was turned off; and the confining pressure pump was now converted to axial loading pump (Figure 2). Axial stress beyond the confining pressure started to apply to the rock sample at the chosen injection rate until end of the test.

Results

This section introduces preliminary results obtained using the new testing method. The first subsection shows the qualitative observation of the tested samples, the induced fractures, and their corresponding axial effective stress-time curves. The second subsection demonstrates the quantitative analyses of the detailed failing/fracturing processes, and the pertaining variation of axial effective stress/axial permeability-time curves of six specimens tested under different confining pressures from 100 to 4,000 psi.

Qualitative observation of confining pressure impact on fracture brittleness

Based on typical features of a tri-axial geomechanics test, the fracture brittleness can be identified qualitatively. Similarly, with a tri-axial core flooding test apparatus, rock matrix permeability, and later fracture conductivity, can be measured and monitored

How to cite this article: Zeng Z, Harouaka A. A New Method for Simultaneously Testing Fracture Brittleness and Conductivity. JOJ Material Sci. 2021; 6(4): 555693. DOI: 10.19080/JOJMS.2021.06.555693

under given reservoir in-situ stresses, pore pressure and temperature conditions. To demonstrate the proposed technology, a series of flooding and fracturing tests under different confining pressures were conducted [38]. These tests were carried out on Indiana limestone samples using an in-house developed fluid-rock interaction dynamics (FRID) testing facility [35]. Some of the testing results were interpreted in terms of brittle fracturing and ductile swelling, as well as their impact on matrix and fracture permeability. Figure 4 shows the axial stress loading curves and failed specimens of five tests under different confining pressures varying from 30 psi to 4,000 psi. In this figure, Indiana limestone experienced brittle fracture when the confining pressure was lower than 1,000 psi; it demonstrated ductile failure when the confining pressure was higher than 2,000 psi. The tested samples, under brittle failure mode, showed a near vertical fracture. In contrast, in ductile failure, near horizontal fractures were formed when confining pressures were 2,000 psi and 3,000 psi. When confining pressure was 4,000 psi, conjugating compaction bands were observed on the failed sample.

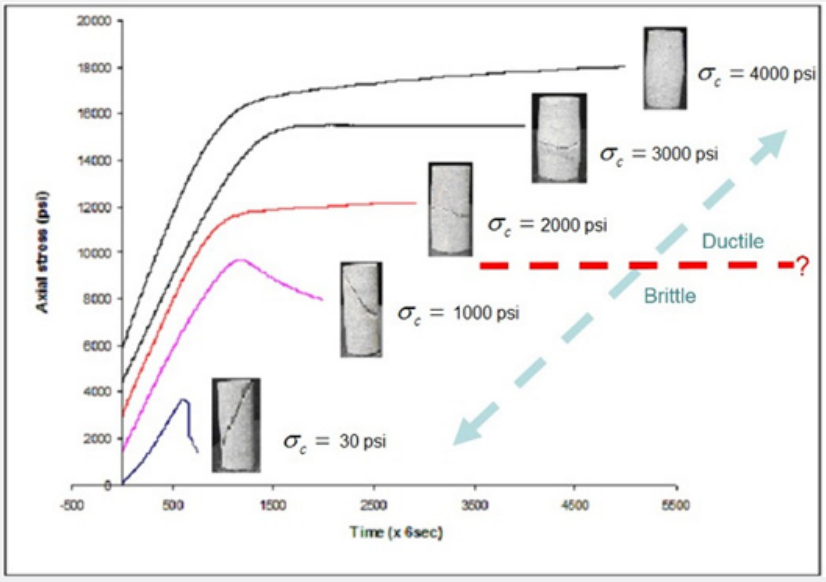

Figure 4: Indiana limestone failure mode changes from brittle fracturing to ductile swelling with the increase of confining pressure from 30 psi to 4,000 psi [38].

Quantitative analysis of fracture brittleness and fracture conductivity

Figure 4 shows that axial stress-time curves recorded in this testing system can be used to identify if the rock sample would fracture/fail in brittle or ductile mode, or a mode in-between, i.e. semi-brittle or semi-ductile mode. The post-peak fracture brittleness is further confirmed by the induced fractures geometry and orientation. These observations are consistent with results by others [23,39]. Clearly, the difference in fracture geometry would have a big impact on the induced fracture conductivity. This is further investigated quantitatively through in-depth analyses of six tests as shown below.

Specimen 1: confining pressure = 100 psi (Sample 10IL08)

Specimen 1 was tested under a confining pressure of 100 psi. Figure 5 shows the time history of axial effective stress (blue line, left Y-axis) and axial permeability (pink line, right Y-axis) during the fracturing process. Based on Figure 4 under a confining pressure of 100 psi, Indiana limestone experienced brittle fracturing. The time history of the axial effective stress and axial permeability in Figure 5 showed the details of this process. Following the classic description of the relationship between micro-cracking and axial stress in tri-axial compression [40], five vertical lines (green) were added onto Figure 5 to divide the whole process into 6 stages from A to F. The following analysis and interpretation aims to establish a correlation between axial permeability and axial effective stress in the process of rock failing/fracturing, thus demonstrating the relationship between rock mechanical dynamics and fluid hydraulic dynamics.

At Stage A in Figure 5, axial effective stress was gradually increased. The rock specimen experienced linear compression, and the axial permeability experienced a slight decrease. During Stage B, the compression continued, and the rock specimen shifted from random micro-cracking to fracture nucleation. The trend of axial permeability reverted from decreasing to increasing at a very slow rate.

During Stage C, the axial effective stress climbed approaching its peak, and then dropped down at free fall pace; all occurred in

How to cite this article: Zeng Z, Harouaka A. A New Method for Simultaneously Testing Fracture Brittleness and Conductivity. JOJ Material Sci. 2021; 6(4): 555693. DOI: 10.19080/JOJMS.2021.06.555693

a very short period. This free fall corresponded to the breakdown instance of fracturing. The peak value of the axial effective stress allows the determination of breakdown pressure [30]. The axial permeability, on the other hand, experienced a vertical jump up corresponding to the free fall drop of the axial effective stress. The axial effective stress and the axial permeability changed simultaneously, but in the opposite trend: when the axial effective stress was slowly approaching its peak at a decelerating pace, the axial permeability was increasing at an accelerating pace. When the axial effective stress decreased vertically in free fall, the axial permeability increased vertically at an extreme (infinite) rate.

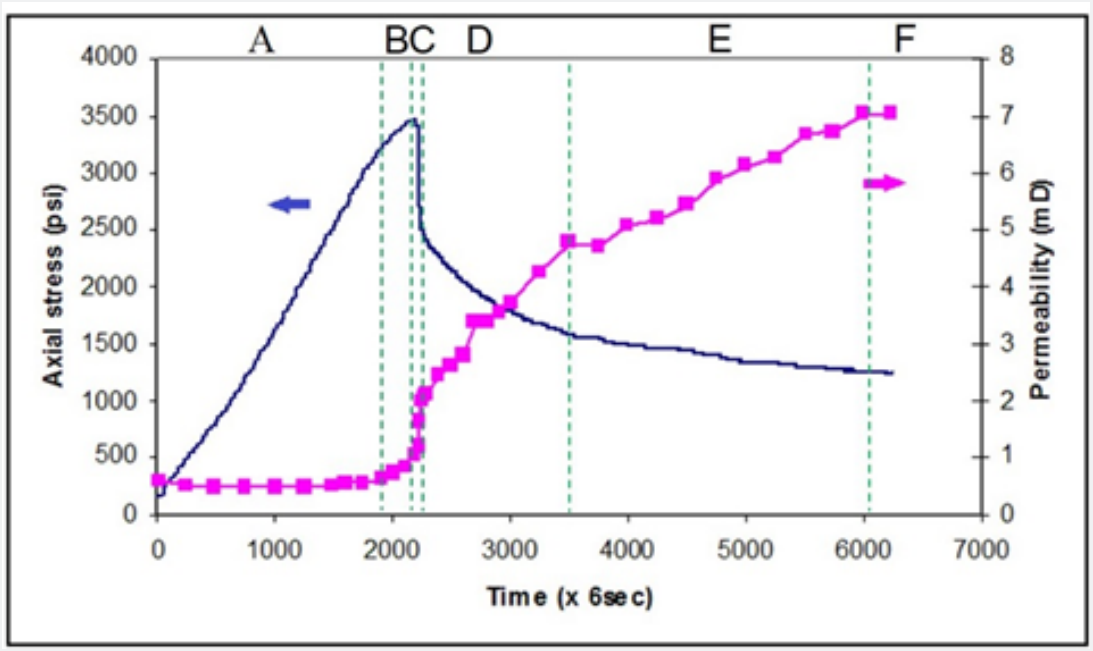

Figure 5: Specimen 1 axial permeability variation corresponding to axial effective stress change during fracturing of Indiana limestone under 100 psi confining pressure.

The free fall change of the axial effective stress indicated a perfect brittle fracturing process; the axial permeability dynamics depictured the fluid transportation behavior from matrix seepage to "channel" flow in the fracture (from Darcian to flow in pipes). From this point on, the matrix permeability is dominated by the fracture permeability. While it is possible to use the volumetric variation of the specimen before and after the breakdown period to assess the fracture "width," and thus the fracture conductivity, it would be more practical and convenient to simplify the non-proppanted fracture "width" as unit. This way the variation of fracture permeability can represent that of the fracture conductivity [41].

Stage D started after breakdown. The axial effective stress continued to decrease, non-linearly, at a rapid pace. The axial permeability shifted from a very sudden increase to a linear rapid growth. The newly formed fracture was in its settling down process.

Stage E started when the slope of the axial effective stress became clearly smaller/flatter and more linear than those in Stage D. The corresponding axial permeability was still growing linearly, with a slower slope. Stage E could be considered as a continued settling down process of the fracture, except that it was at a slower progression. At the end of Stage E, axial effective stress reached a constant value, which represented the residual strength of Indiana limestone at that confining pressure. This was the beginning of Stage F. Figure 5 showed that both axial effective stress and axial permeability became stabilized during Stage F.

Specimen 2: confining pressure = 300 psi (Sample 09IL06)

Specimen 2 was tested under a confining pressure of 300 psi. Figure 6 shows the results pertaining to axial effective stress and axial permeability measured simultaneously. Comparing to Specimen 1 depicted in Figure 5, the fracturing process in Figure 6 was less brittle. In addition, the following observations were made:

a) Stage A, axial permeability continuously decreased with increase in axial effective stress. This is in contrast with that shown in Figure 5.

b) Stage B, the relationship between the axial permeability and the change in axial effective stress was like Figure 5, indicating enhancement of axial permeability due to micro-cracking.

How to cite this article: Zeng Z, Harouaka A. A New Method for Simultaneously Testing Fracture Brittleness and Conductivity. JOJ Material Sci. 2021; 6(4): 555693. DOI: 10.19080/JOJMS.2021.06.555693

c) Stage C, axial effective stress decreased gradually while axial permeability increased steadily; this was quite different from the breakdown process in Specimen 1 (Figure 5). It indicated that Specimen 2 experienced a less brittle breakdown.

d) Stage D, the relationship between axial permeability and axial effective stress was similar to that seen in Figure 5, except the axial permeability of Specimen 2 increased much slower and reached a much lower value than their counterparts in Specimen 1.

e) Stage E, both axial effective stress and axial permeability decreased steadily, contrasting to the behavior observed in Figure 5.

f) Stage F, both Specimens 1 and 2 were similar.

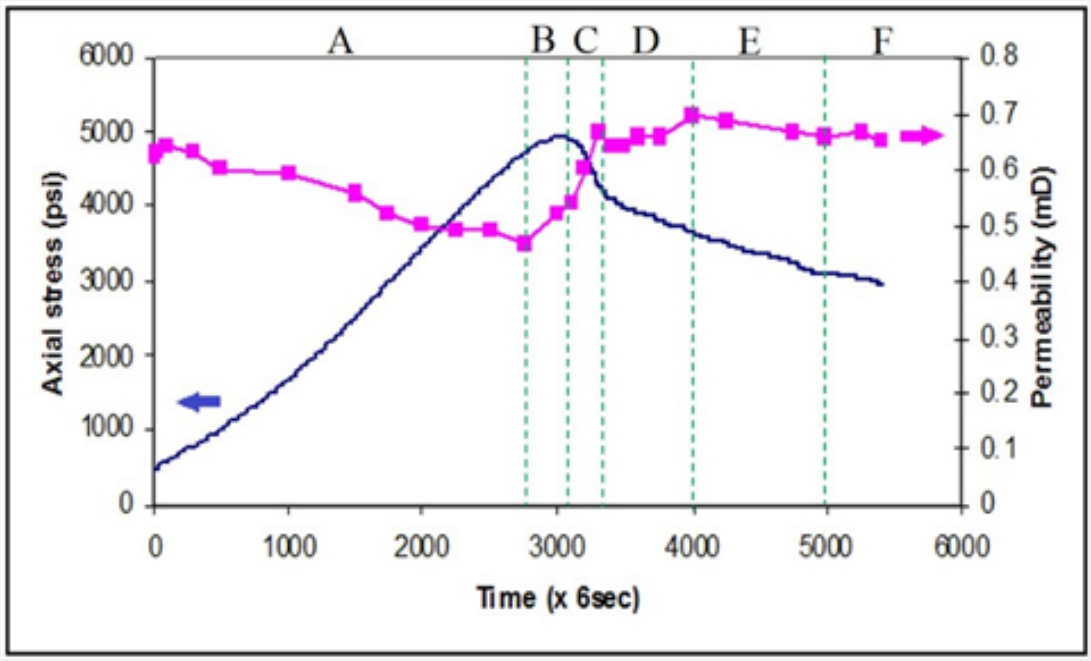

Figure 6: Specimen 2 axial permeability variation corresponding to axial effective stress change during the fracturing of Indiana limestone under 300 psi confining pressure.

Briefly, the initial matrix permeability in Specimens 1 & 2 were both about 0.7 mD. In Specimen 1 (Figure 5) the fracture permeability had increased 10+ folds to a value of 7 mD. In contrast, the permeability in Specimen 2 (Figure 6) decreased first to about 0.4 mD, and then recovered to about 0.7 mD after fracturing. The fracturing did not improve the permeability in this case.

Specimen 3: confining pressure = 1,500 psi (Sample 08IL92)

Testing on Specimen 3 was conducted under a confining pressure of 1,500 psi. Figure 7 shows the time history of axial effective stress and axial permeability during the compression and fracturing process. The overall axial effective stress curve showed a brittle breakdown process. The axial permeability curve showed monotonic decrease except during the breakdown stage.

In comparison to Specimen 1, the axial effective stress showed similar behavior, including a sudden drop of axial effective stress in Stage C. However, careful comparison indicated that in Stage C of Specimen 3, the sudden drop of axial effective stress occurred after the peak stress, indicating that the breakdown itself was progressive, and there was a small-scale brittle cracking post-breakdown. In addition, the axial effective stress in the residual stage did not decrease; it rebounded slightly and maintained that rebound to the end, which was interpreted as a representation of some sort of ductile behavior; this was quite different from Specimen 1.

The axial permeability revealed quite different behavior when compared to that of Specimen 1. The axial permeability monotonically decreased in all Stages except C. In Stage C the axial permeability experienced a small ripple corresponding to the post-peak brittle cracking. Overall, the axial permeability decreased from the initial value of 4 mD to a final value of 2.4 mD. The brief brittle cracking caused a temporary increase in permeability but did not enhance the overall fracture permeability.

Specimen 4: confining pressure = 2,200 psi (Sample 08IL95)

Specimen 4 was tested under a confining pressure of 2,200 psi. The axial effective stress curve (Figure 8) was like Specimen 3 (Figure 7), with a post-peak brief brittle cracking. However, the axial effective stress in the residual stages (D, E and F) increased slowly and steadily. The axial permeability was also like Specimen 3 except for that in Stage C. Although there was a post-peak brief

How to cite this article: Zeng Z, Harouaka A. A New Method for Simultaneously Testing Fracture Brittleness and Conductivity. JOJ Material Sci. 2021; 6(4): 555693. DOI: 10.19080/JOJMS.2021.06.555693

brittle cracking in Figure 8 as that seen in Figure 7 (Specimen 3), the axial permeability corresponding to this brittle cracking was a sudden decrease, opposite to that seen in Figure 7. Overall, the axial permeability of Specimen 4 decreased monotonically from about 6.5 mD to the end value of about 2.8 mD. Results in Specimen 4 indicated that mechanical dynamic behavior could be inconsistent with, or even opposite to, the hydraulic dynamic behavior of the fracture, under this confining pressure.

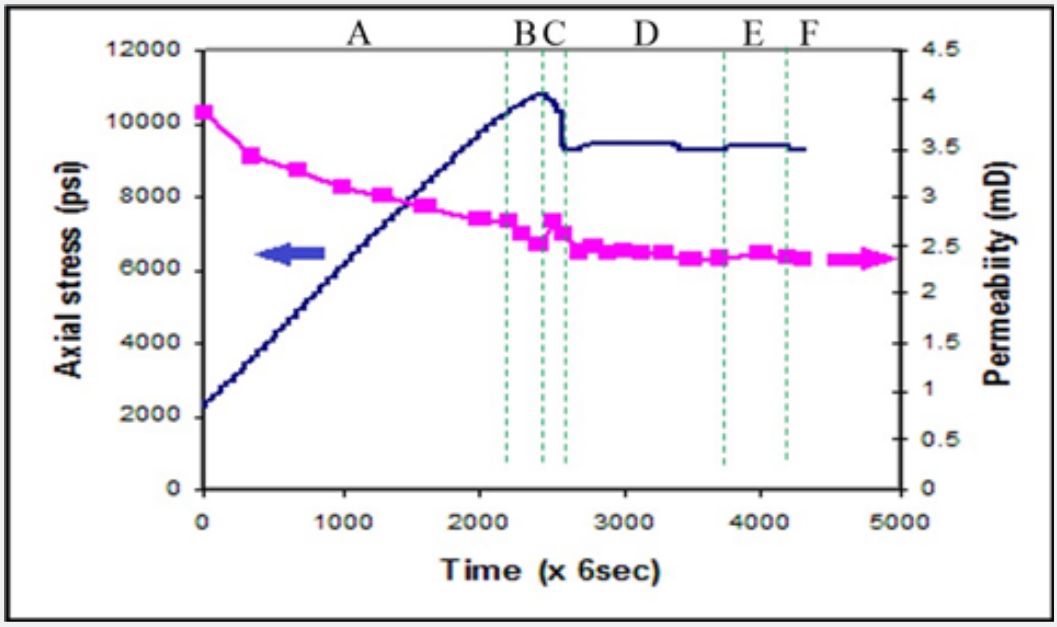

Figure 7: Specimen 3 axial permeability variation corresponding to axial effective stress change during the fracturing of Indiana limestone under 1,500 psi confining pressure.

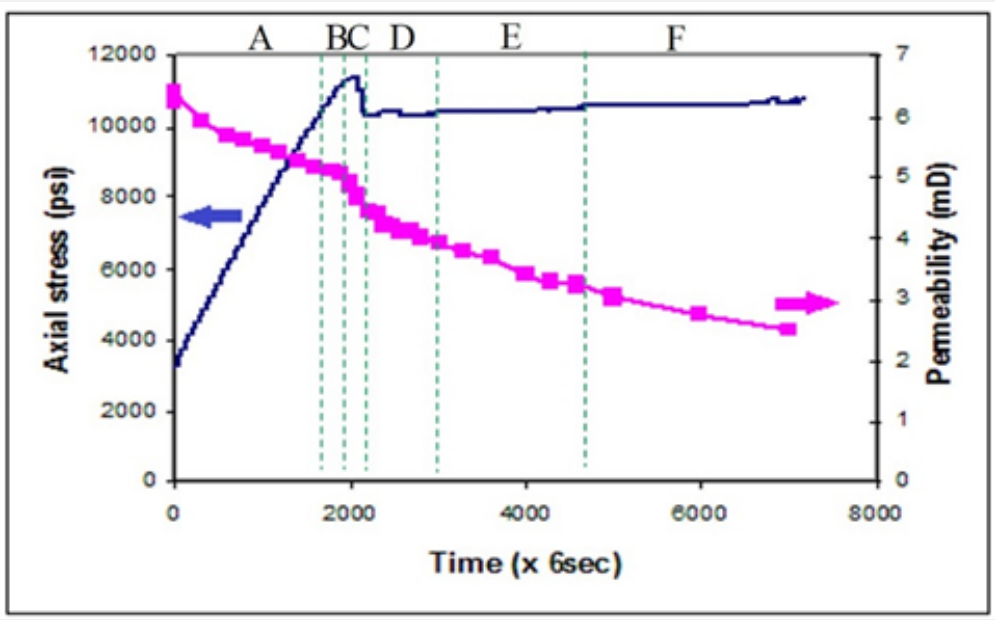

Figure 8: Specimen 4 axial permeability variation corresponding to axial effective stress change during the fracturing of Indiana limestone under 2,200 psi confining pressure.

Specimen 5: confining pressure = 3,000 psi (Sample 08IL12)

Testing on Specimen 5 was conducted at a confining pressure of 3,000 psi (Figure 9). When compared to Specimen 4 (Figure 8), the axial effective stress showed similar behavior except in Stage C (Figure 9); Specimen 5 showed progressive, steady failure. There was less brittle behavior in the breakdown stage. The trend of

How to cite this article: Zeng Z, Harouaka A. A New Method for Simultaneously Testing Fracture Brittleness and Conductivity. JOJ Material Sci. 2021; 6(4): 555693. DOI: 10.19080/JOJMS.2021.06.555693

axial permeability was like that in Specimen 4, showing monotonic decrease during the whole process except for some brief ripples. Overall, the axial permeability of Specimen 5 decreased from an initial value of 5.5 mD to a final value of about 1.5 mD.

Specimen 6: confining pressure = 4,000 psi (Sample 08IL11)

Testing on Specimen 6 was performed under a confining pressure of 4,000 psi. When compared to all the previous specimens (Figures 5-9), Specimen 6 showed completely ductile failing behavior (Figure 10). There was no sign of fracturing. The whole process could be vaguely divided into two stages, i.e. A and F. Accompanying a monotonic increase and flattening in axial effective stress, the axial permeability decreased monotonically, and reduced to zero when the deformation entered Stage F. Overall axial permeability of Specimen 6 reduced from an initial value of about 0.55 mD to zero at the residual stage.

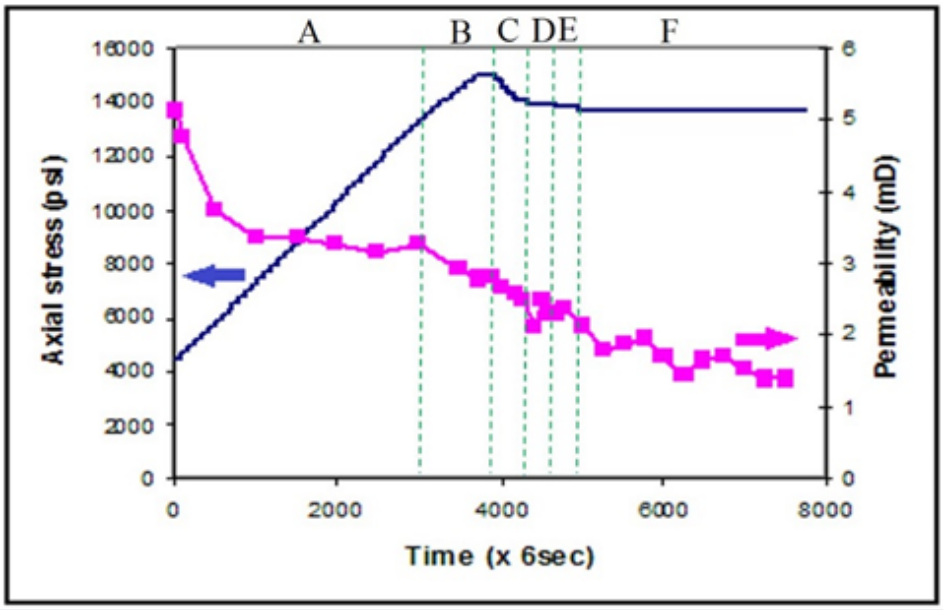

Figure 9: Specimen 5 axial permeability variation corresponding to axial effective stress change during the fracturing of Indiana limestone under 3,000 psi confining pressure.

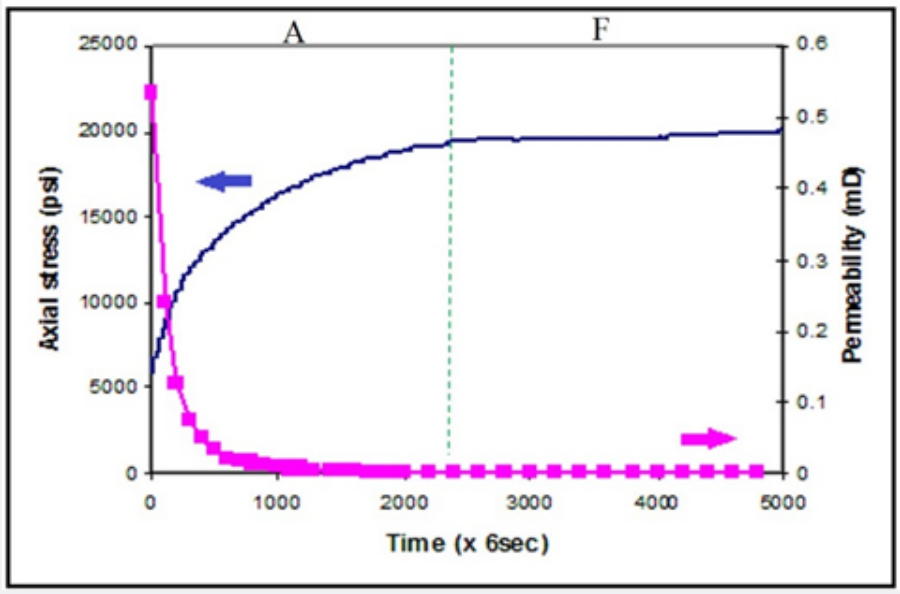

Figure 10: Specimen 6 axial permeability variation corresponding to axial effective stress change during the failing of Indiana limestone under 4,000 psi confining pressure.

How to cite this article: Zeng Z, Harouaka A. A New Method for Simultaneously Testing Fracture Brittleness and Conductivity. JOJ Material Sci. 2021; 6(4): 555693. DOI: 10.19080/JOJMS.2021.06.555693

Discussion

From the analysis of these tests, it can be seen that there exists a complicated relationship between the rock mechanical dynamics and the hydraulic dynamics of the deformed/fractured/failed Indiana limestone samples used in this work. Confining pressure has a big impact on the deformation and failure mode of Indian limestone, which further affects the permeability behavior.

Under low confining pressures, the rock samples analyzed experienced brittle fracture, leading to conductive fractures. The axial permeability was enhanced by the fracturing process. Under high confining pressures, the rock samples analyzed experienced ductile failing. In this case, conjugate deformation bands were initiated, and the axial permeability was either decreased, or completely lost. When the confining pressures were in the intermediate range, the rock behavior was partially brittle (at the breakdown stage), and partially ductile (at the residual stage). The permeability could be temporarily or permanently enhanced, depending on the fracturing process.

In the real world, the tight oil formation rocks, such as those in Wolfcamp formation, Permian Basin, USA are most likely to be under the confining pressure of the intermediate range [5]. From these tests and the range of confining pressures studied, brittle fracturing in the breakdown stage may not guarantee the creation of conductive fractures. A ductile behavior in the residual stage could easily reverse the fracture permeability gained in the brittle breakdown stage. Consequently, one should not be surprised by seeing that some HF stimulations might have a brittle breakdown stage from the mechanical performance, but still fail to provide the type of expected fracture conductivity.

Reservoir pressure is higher than the pressure used in the tests in this paper. It is found that high pore pressure would convert a rock from ductile failing to brittle fracturing [23]. From this perspective, results obtained under lower reservoir (pore) pressure favors the objective of the new testing technology. Similarly, reservoir temperature is usually higher than room temperature used in the tests of this paper. High temperature tends to change the rock toward behaving in ductile mode [23]. For instance it was observed that a rock sample fractured in brittle mode at room temperature of 20°C (68°F) may experience ductile mode at 300°C (572°F) [22]. In general, oil reservoir temperature is below 150°C (302°F), and gas reservoir is below 260°C (500°F), beyond which the hydrocarbon is burnt [42]. From application point of view, results observed under room temperature should cover most oil reservoir rocks. On the other hand, the core-holder and the oven system can support temperature up to 177°C (350°F) if needed [35].

Conclusion

From the study summarized in this paper, the following conclusions have been drawn:

a) A new laboratory testing procedure is proposed to screen for brittle fracturing processes using integrated techniques from tri-axial geomechanics compression, core flooding and poly-axial hydraulic fracturing which allows one to measure fracture brittleness and fracture conductivity simultaneously.

b) Formation rocks can be tested using this method under given reservoir in-situ stresses and pore pressure, temperature, as well as HF fluid properties, to exclude (reduce) the possibilities of ductile failure (swelling and flow), and to increase the likelihood of brittle fracturing.

c) Tests on Indiana limestone show that confining pressure has a big impact on failure modes. At low confining pressures, Indiana limestone undergoes brittle failure (fracturing), which greatly enhances the permeability. At high confining pressures, Indiana limestone undergoes ductile failure (swelling and plastic flowing), which greatly reduces the permeability. At the intermediate confining pressures, Indiana limestone undergoes brittle behavior at the breakdown stage, and ductile behavior at the residual stage. The permeability might be enhanced temporarily at the brittle breakdown stage but might eventually be lost completely at the residual stage.

d) Most real-world reservoir rocks in Wolfcamp formation, Permian Basin, USA are under the intermediate confining pressure range. This greatly increases the risk of creating a non-conductive fracture though there is a brittle breakdown stage.

e) Future effort to apply this method on different rocks under more representative reservoir conditions, such reservoir pressure will improve its applicability and potential.

Acknowledgement

This work is partly supported by UT STARs program (Project P5011236-23) of University of Texas System, Texas, USA.

References

1. NETL (2011) Shale Gas: Applying Technology to Solve America's Energy Challenges. National Energy Tech Lab (NETL) U.S. Dept of Energy p. 1-8.
2. Schrider LA, Wise RL (1980) Potential new sources of natural gas. J Pet Technol 32(4): 703-716.
3. Price LC, Lefever J (1994) Dysfunctionalism in the Williston Basin: the Bakken/mid-Madison petroleum system. Bulletin of Canadian Petroleum Geology 42(2): 187-218.
4. King GE (2010) Thirty years of gas fracturing: what have we learned? Paper SPE133456 presented at The SPE Annual Technical Conference and Exhibition held in Florence, Italy, September p. 19-22.
5. Zeng Z, Harouaka A (2020) A new method for assessing stage-based hydraulic fracturing quality in Wolfcamp formation of Permian Basin. J Petrol Sci and Eng 195: 107740.
6. Howard GC, Fast CR (1970) Hydraulic Fracturing. Soc Petrol Engin Richardson Texas USA p. 1-10.

How to cite this article: Zeng Z, Harouaka A. A New Method for Simultaneously Testing Fracture Brittleness and Conductivity. JOJ Material Sci. 2021; 6(4): 555693. DOI: 10.19080/JOJMS.2021.06.555693

7. Economides MJ, Nolte KG (1989) Reservoir Stimulation (2nd edn.). Schlumberger Educational Services, Houston, Texas, USA p. 23-44.

8. Veatch RW Jr, Moschovidis ZA, Fast CR (1989). Chapter 1 An overview of hydraulic fracturing. In: Gidley JL, et al. (eds.). Recent Advances in Hydraulic Fracturing. Society of Petroleum Engineers, Richardson, Texas, USA p. 1-38.

9. Economides MJ, Nolte KG (2000) Reservoir Stimulation (3rd edn.), John Wiley & Sons Ltd Chichester, England, UK, p. 29-473.

10. Pendleton LE (1991) Horizontal drilling review. Paper SPE23535 presented at the Second Archie Conference held in Houston, Texas, USA, November p. 3-6.

11. Reiss LH (1987) Production from horizontal wells after 5 years. J Pet Technol 39(11): 1411-1416.

12. Joshi SD (1987) A review of horizontal well and drain-hole technology. Paper SPE16868 presented at the 62nd Annual Tech Conf & Exhib Soc Petrol Engin held in Dallas, Texas, USA, p. 27-30.

13. Strubhar MK, Fitch JL, Glenn EE Jr (1975) Multiple, vertical fractures from an inclined wellbore - a field experiment. J Pet Technol 27(5): 641-647.

14. Roegiers JC, Detournay E (1988) Considerations on fracture initiation in inclined borehole. In: Cundall (eds.), Key Questions in Rock Mechanics, Proc 29th US Symp Rock Mech AA Balkeman, Rotterdam, The Netherlands, pp. 461-469.

15. Scott TE, Zeng Z, Roegiers JC (2000) Acoustic emission imaging of induced asymmetrical hydraulic fractures. Paper ARMA/NARMS 04-562 presented to the 6th North America Rock Mechanics Symposium, Houston, Texas, USA.

16. McLennan JD, Roegiers JC, Economides MJ (1990) Chapter 19 Extended reach and horizontal wells. In: Economides MJ & Nolte KG (eds.) Reservoir Stimulation (2nd ed.). Schlumberger Educational Services, Houston, Texas, USA, pp. 361-388.

17. LaFollette RF, Holcomb WD, Aragon J (2012) Practical Data Mining: Analysis of Barnett Shale Production Results with Emphasis on Well Completion and Fracture Stimulation. Paper SPE-152531 presented at the SPE Hydraulic Fracturing Tech. Conf., The Woodlands, Texas, USA, p. 6-8.

18. Jin X, Shah SN, Roegiers JC, Zhang B (2015) An integrated petrophysics and geomechanics approach for fracability evaluation in shale reservoirs. SPE J 20(3): 518-526.

19. Smith MB, Hannah RR (1996) High-permeability fracturing: The evolution of a technology. J Pet Technol 48(7): 628-633.

20. El Rabba AM, Shah SN, Lord DL (1999) New perforation pressure-loss correlations for limited-entry fracturing treatments. SPE Prod & Fac 14: 63-71.

21. Zeng Z, Roegiers JC, Grigg R (2003) Imaging the initiation of asymmetrical hydraulic fractures in laboratory experiments. Paper SPE-84578-MS Presented at the SPE Annual Technical Conference and Exhibition, Denver, Colorado, USA October p. 5-8.

22. Hu L, Ghassemi A, Pritchett J, Garg S (2020) Characterization of laboratory-scale hydraulic fracturing for EGS. Geothermics 83:101706.

23. Jaeger JC, Cook NGW (1979) Fundamentals of Rock Mechanics (3rd edn.). London: Chapman and Hall, pp. 81-280.

24. Terzaghi K (1945) Stress conditions for the failure of saturate concrete and rock. A S T M Proc 45: 777-792.

25. Griggs D, Handin J (1960) Observations on fracture and a hypothesis of earthquakes. In: Griggs & Handin (eds.) Rock Deformation. GSA Memoir 79: 347-373.

26. Vutukuri VS, Lama RD, Saluja SS (1974) Handbook on Mechanical Properties of Rocks. Trans Tech Publications, Clausthal, Germany 1: 216-219.

27. Fjar E, Holt RM, Raaen AM (2008) Petroleum-related Rock Mechanics. Elsevier Science Publish, Amsterdam, The Netherlands, pp. 55-433.

28. Roegiers JC (1990) Chapter 2 Elements of rock mechanics. In: Economides MJ, Nolte KG (eds.), Reservoir Stimulation (2nd ed.). Schlumberger Educational Services, Houston, Texas, USA.

29. Abass HH, Hedayati S, Meadows DL (1996) Nonplanar Fracture Propagation from a Horizontal Wellbore: Experimental Study. SPE Prod & Fac 11(3): 133-137.

30. Zeng Z, Roegiers JC (2002) Experimental observation of injection rate influence on the hydraulic fracturing behavior of a tight gas sandstone. Paper SPE 78172 presented to SPE/ISRM Rock Mechanics Conference, Irving, Texas, USA.

31. Zeng Z (2009) Imaging Hydraulic Fracturing: Analytical Solution, Numerical Modeling and Lab Testing. VDM-Publishing, Saarbrücken, Germany, pp. 33-53.

32. Tiab D, Donaldson EC (2004) Petrophysics (2nd edn.), Gulf Publishing Company, Houston, Texas, USA, pp. 813-822.

33. Zhang J, Kamenov A, Zhu D, Hill AD (2014) Laboratory measurement of hydraulic-fracture conductivities in the Barnett shale. SPE Prod & Oper 29(3): 216-227.

34. Zeng Z, Grigg RB, Roegiers JC (2004) Experimental determination of geomechanical and petrophysical properties of Jackfork sandstone - a tight gas formation. Paper ARMA/NARMS 04-562 presented to the 6th North America Rock Mechanics Symposium, Houston, Texas, USA.

35. Zeng Z, Jakupi A, Bigelow T, Kringstad J, Belobraydic M, et al. (2008) Laboratory observation of CO_2 phase transition induced seismic velocity change. Paper ARMA 08-329 presented to the 42nd US Rock Mechanics Symposium, San Francisco, California, USA.

36. ISRM (1983) Suggested Methods for Determining the Strength of Rock Materials in Triaxial Compression: Revised Version. International Society for Rock Mechanics (ISRM) 20(6): 285-290.

37. Fairhurst CE, Hudson JA (1999) Draft ISRM suggested method for the complete stress-strain curve for intact rock in uniaxial compression. Int J Rock Mech & Mining Sci 36: 279-289.

38. Zhou XJ, Zeng Z, Liu H (2011) Stress-dependent permeability of carbonate rock and the implication to CO_2 sequestration. Paper ARMA 11-135 presented to the 45th US Rock Mechanics / Geomechanics Symposium, San Francisco, California, USA.

39. Paterson MS, Wong TF (2005) Experimental Rock Deformation - The Brittle Field (2nd edn.), Springer, The Netherlands, p. 5-237.

40. Hallbauer DK, Wagner H, Cook NGW (1973) Some observations concerning the microscopic and mechanical behavior of quartzite specimens in stiff, tri-axial compression tests. Int J Rock Mech Min Sci 10(6): 713-726.

41. Veatch RW, King GE, Holditch SA (2017) Essentials of Hydraulic Fracturing: Vertical and Horizontal Wellbores. PennWell Corporation, Tulsa, Oklahoma, USA, pp. 7-197.

42. PETEX (2011) Fundamentals of Petroleum. The University of Texas at Austin Petroleum Extension (PETEX), Austin, Texas USA, p. 25-29.

How to cite this article: Zeng Z, Harouaka A. A New Method for Simultaneously Testing Fracture Brittleness and Conductivity. JOJ Material Sci. 2021; 6(4): 555693. DOI: 10.19080/JOJMS.2021.06.555693

DOI: 10.19080/JOJMS.2020.06.555693

How to cite this article: Zeng Z, Harouaka A. A New Method for Simultaneously Testing Fracture Brittleness and Conductivity. JOJ Material Sci. 2021; 6(4): 555693. DOI: 10.19080/JOJMS.2021.06.555693